Inorg. Chem. **1993**, *32*, 5756–5761

A New Linkage Isomer of RhCl$_3$(DMSO)$_3$: Photochemical Synthesis, Crystal Structure, and Reactivity of *mer,trans*-RhCl$_3$(DM*S*O)$_2$(DMS*O*)

Enzo Alessio,* Paolo Faleschini, Andrea Sessanta o Santi, Giovanni Mestroni, and Mario Calligaris

Dipartimento di Scienze Chimiche, Università di Trieste, 34127 Trieste, Italy

Received June 18, 1993⊗

The photochemical isomerization of *mer,cis*-RhCl$_3$(DM*S*O)$_2$(DMS*O*) (**1**) to the new linkage isomer *mer,trans*-RhCl$_3$(DM*S*O)$_2$(DMS*O*) (**2**) is described. The new isomer has been characterized by spectroscopic techniques and three-dimensional X-ray analysis. Crystal data: monoclinic, $P2_1/c$, $a = 10.123(6)$ Å, $b = 13.557(2)$ Å, $c = 11.109(5)$ Å, $\beta = 94.49(2)°$, $Z = 4$, $R = 0.048$. This is the first case where the crystal structures of two DMSO linkage isomers are known. Complex **2** is thermodynamically unstable compared to **1**, and in solution of aprotic solvents it slowly isomerizes with first-order kinetics. The two isomers react stereospecifically with nitrogen ligands by following different paths and produce isomeric products.

Introduction

Rhodium–chloride–dimethyl sulfoxide complexes of general formula $[\mathrm{RhCl}_n(\mathrm{DMSO})_{6-n}]^{3-n}$ (n = 0–5) have been studied since the late sixties.[1–9] Particular attention has been devoted to the monoanionic (n = 4) and neutral (n = 3) members of the series, since they are more easily synthesized from hydrated RhCl$_3$. They have found applications as starting materials in inorganic syntheses[3,9–13] and as catalyst precursors in several processes, such as air oxidation of sulfoxides to sulfones,[2,6] hydrogenolysis of O$_2$ to H$_2$O$_2$,[14] and olefin polymerization reactions.[15]

Dimethyl sulfoxide can bind to rhodium(III) either through the sulfur atom (DM*S*O) or through the oxygen atom (DMS*O*). As a general rule, DMS*O* has a preference to be trans to DM*S*O and the number of O-bonded sulfoxides increases upon increasing the positive charge on the rhodium atom.[8] These features have been confirmed in the crystal structures of X[*trans*-RhCl$_4$(DM*S*O)$_2$] (X$^+$ = Na$^+$,[16] (DMSO)$_2$H$^+$,[17] (C$_{14}$H$_{17}$N$_2$)$^+$ and (C$_{14}$H$_{19}$N$_2$)$^+$,[18] (NEt$_2$H$_2$)$^+$ [19]), *mer,cis*-RhCl$_3$(DM*S*O)$_2$(DMS*O*),[20] and *trans,cis,cis*-[RhCl$_2$(DM*S*O)$_2$(DMS*O*)$_2$][BF$_4$].[21]

Beside X-ray crystallography, the mode of binding of DMSO on Rh(III) has been investigated by vibrational[1,4,7,8] and NMR spectroscopy.[8,9,22] Detailed NMR studies[8,9] showed that almost every derivative of the above series could exist as more than one isomer in solution. The isomers might differ from each other both in the geometry and in the mode of binding of the DMSO ligands (linkage isomers). In the case of the neutral derivative, *mer,cis*-RhCl$_3$(DM*S*O)$_2$(DMS*O*) (**1**), the establishment of a rapid equilibrium with an all S-bonded species *mer*-RhCl$_3$(DM*S*O)$_3$ was proposed to account for the two minor peaks (3.51 and 3.50 ppm, intensity 2:1) that are found in the S-bonded DMSO region of the CDCl$_3$ ^{1}H NMR spectrum.[8,9] An additional minor isomer with at least one O-bonded DMSO was reported to grow slowly with time.[8,9] Attempts to isolate the isomers by repeated crystallizations or chromatographic separations were unsuccessful.[9]

In our extensive studies on ruthenium–DMSO complexes[23–25] we observed remarkable structural analogies between the Ru(III) (d^5) and Rh(III) (d^6) series of general formula $[\mathrm{MCl}_n(\mathrm{DMSO})_{6-n}]^{3-n}$, for n = 3 and 4. Interestingly, while the anionic Ru(III) complex *trans*-[RuCl$_4$(DM*S*O)$_2$]$^-$ is isostructural[24,26] to the Rh analogue, the neutral derivative *mer,trans*-RuCl$_3$(DM*S*O)$_2$(DMS*O*) is an isomer of the rhodium counterpart **1**, the two DM*S*O ligands being trans instead of cis to each other.[24] We had also reported the light-induced isomerization of *cis,fac*-RuCl$_2$(DM*S*O)$_3$(DMS*O*) to the less thermodynamically stable isomer *trans*-RuCl$_2$(DM*S*O)$_4$.[23] These results prompted us to investigate the effect of light on the equilibria between the neutral Rh–DMSO isomers.

Experimental Section

Material. Analytical grade dimethyl sulfoxide (C. Erba) and solvents (Baker) were used without further purification for synthetic purposes. RhCl$_3$·3H$_2$O was purchased from Johnson Mattey. 1,5,6-Trimethylbenzimidazole was synthesized from 5,6-dimethylbenzimidazole (Aldrich) as reported.[27] Deuterated solvents for NMR were purchased from Aldrich and Cambridge Isotope Laboratories.

⊗ Abstract published in *Advance ACS Abstracts*, November 1, 1993.

(1) Johnson, B. F. G.; Walton, R. A. *Spectrochim. Acta* **1966**, *22*, 1853.
(2) Trocha-Grimshaw, J.; Henbest, H. B. *J. Chem. Soc., Chem. Commun.* **1968**, 1035.
(3) Kukushkin, Yu. N.; Rubtsova, N. D. *Russ. J. Inorg. Chem.* **1969**, *14*, 980.
(4) Kukushkin, Yu. N.; Rubtsova, N. D. *Russ. J. Inorg. Chem.* **1969**, *14*, 1115.
(5) Kukushkin, Yu. N.; Rubtsova, N. D.; Ivannikova, N. V. *Russ. J. Inorg. Chem.* **1970**, *15*, 1032.
(6) Henbest, H. B.; Trocha-Grimshaw, J. *J. Chem. Soc., Perkin Trans.* **1974**, 607.
(7) Faadev, Yu. V.; Kukushkin, Yu. N.; Khokhryakov, K. A. *Russ. J. Inorg. Chem.* **1975**, *20*, 1519.
(8) Barnes, J. R.; Goggin, P. L.; Goodfellow, R. J. *J. Chem. Res. Miniprint* **1979**, 1610.
(9) James, B. R.; Morris, R. H. *Can. J. Chem.* **1980**, *58*, 399.
(10) Rochon, F. D.; Kong, P. C.; Melanson, R. *Can. J. Chem.* **1983**, *61*, 1823.
(11) Smeets, W. J. J.; Spek, A. L.; Niele, F. G. M.; Mertens, C. F.; Nolte, R. J. M. *Acta Crystallogr.* **1987**, *C43*, 2330.
(12) Gamage, S. N.; Morris, R. H.; Rettig, S. J.; James, B. R. *J. Organomet. Chem.* **1986**, *309*, C59.
(13) Colamarino, P.; Orioli, P. *J. Chem. Soc., Dalton Trans.* **1976**, 845.
(14) Gamage, S. N.; James, B. R. *J. Chem. Soc., Chem. Commun.* **1989**, 1624.
(15) Dass, N. N.; Sen, S. R. *J. Polym. Sci.* **1983**, *21*, 3381.
(16) Sokol, V. I.; Rubstova, N. D.; Gribernyuk, A. Y. *J. Struct. Chem.* **1974**, *15*, 296.
(17) James, B. R.; Morris, R. H.; Einstein, F. W. B.; Willis, A. *J. Chem. Soc., Chem. Commun.* **1980**, 31.
(18) Gamage, S. N.; Morris, R. H.; Rettig, S. J.; Thackray, D. C.; Thorburn, I. S.; James, B. R. *J. Chem. Soc., Chem. Commun.* **1987**, 894.
(19) Gamage, S. N.; James, B. R.; Rettig, S. J.; Trotter, J. *Can. J. Chem.* **1988**, *66*, 1123.
(20) Sokol, V. I.; Porai-Koshits, M. A. *Sov. J. Coord. Chem.* **1975**, *1*, 476.
(21) Calligaris, M.; Faleschini, P.; Alessio, E. *Acta Crystallogr.* **1991**, *C47*, 747.
(22) Fotheringham, J. D.; Heath, G. A.; Lindsay, A. J.; Stephenson, T. A. *J. Chem. Res. Miniprint* **1986**, 801.
(23) Alessio, E.; Mestroni, G.; Nardin, G.; Attia, W. M.; Calligaris, M.; Sava, G.; Zorzet, S. *Inorg. Chem.* **1988**, *27*, 4099.
(24) Alessio, E.; Balducci, G.; Calligaris, M.; Costa, G.; Attia, W. M.; Mestroni, G. *Inorg. Chem.* **1991**, *30*, 609.
(25) Alessio, E.; Balducci, G.; Lutman, A.; Mestroni, G.; Calligaris, M.; Attia, W. M. *Inorg. Chim. Acta* **1993**, *203*, 205.
(26) Jaswal, J. S.; Rettig, S. J.; James, B. R. *Can. J. Chem.* **1990**, *68*, 1808.
(27) Simonov, A. M.; Pozharskii, A. E.; Marianovskii, V. M. *Indian J. Chem.* **1967**, *5*, 81.

0020-1669/93/1332-5756$04.00/0

Physical Measurements. Electronic absorption spectra were recorded in stoppered quartz cells with a Perkin-Elmer Lambda 5 UV/vis spectrophotometer equipped with a thermostat. Unless otherwise stated, spectra were recorded immediately after dissolution of the complexes. Solid-state infrared spectra were obtained as KBr pellets on a Perkin-Elmer 983G spectrometer. ^{1}H and ^{13}C NMR spectra were recorded at 400 and 100.5 MHz, respectively, on a Jeol EX400 FT instrument. All spectra were run at room temperature with tetramethylsilane (TMS) as an internal reference for CD$_2$Cl$_2$ and CDCl$_3$ solutions and sodium 2,2-dimethyl-2-silapentane (DSS) for D$_2$O solutions. Elemental analyses were performed by Dr. Cebulec (Dipartimento Scienze Chimiche, Università di Trieste).

Syntheses of the Complexes. *mer,cis*-RhCl$_3$(DM*S*O)$_2$(DMS*O*) (1). The complex could be synthesized either by reaction of RhCl$_3$·3H$_2$O with DMSO as reported[9] or upon treatment of [(DMSO)$_2$H][*trans*-RhCl$_4$(DM*S*O)$_2$] with an equimolar amount of a silver salt in refluxing DMSO/acetone.[24] The complex was recrystallized from CH$_2$Cl$_2$ by addition of diethyl ether, in order to remove traces of **1**·H$_2$O (see below). Anal. Calcd for C$_6$H$_{18}$Cl$_3$O$_3$RhS$_3$ (M_r = 443.64): C, 16.24; H, 4.08; Cl, 23.97; S, 21.67. Found: C, 16.4; H, 3.96; Cl, 24.2; S, 21.8. Visible spectra (λ_{max}, nm (ϵ, M^{-1} cm^{-1})): in CHCl$_3$ solution, 435 (280); in H$_2$O solution, 430 (275); in DMSO solution, 436.5 (327).

***mer,cis*-RhCl$_3$(DM*S*O)$_2$(H$_2$O) (1·H$_2$O).** As already reported,[9] the aquo derivative of **1**, with the water molecule replacing the O-bonded DMSO, could be occasionally isolated in the synthesis of **1**. The complex is readily soluble in water and scarcely soluble in CHCl$_3$. Anal. Calcd for C$_4$H$_{14}$Cl$_3$O$_3$RhS$_2$ (M_r = 383.54): C, 12.52; H, 3.68; S, 16.72. Found: C, 12.4; H, 3.61; S, 17.1. ^{1}H NMR spectrum in CDCl$_3$: 3.68 (s, 6), 3.50 ppm (s, 6). ^{1}H NMR spectrum in D$_2$O: 3.61 (s, 6), 3.45 ppm (s, 6). Selected IR absorption bands (KBr): ν_{SO} 1145, 1110 cm^{-1} (vs, DM*S*O); ν_{Rh-S} 426 cm^{-1} (m); ν_{Rh-Cl} 350 cm^{-1} (s).

***mer,trans*-RhCl$_3$(DM*S*O)$_2$(DMS*O*) (2).** A 0.4-g amount of **1** was dissolved in 45 mL of acetone by gentle warming. The light orange solution was then exposed to sunlight for 3 h. The final, orange-red solution was evaporated to 15 mL without warming and then cooled to 4 °C. Deep-red crystals of the product formed within a few hours; precipitation could be hastened and increased by addition of small amounts of diethyl ether. The crystals were filtered off, rapidly washed with cold acetone and diethyl ether, and vacuum dried (yield 50%). Exposure of the solution of **1** to the light of two 150-W bulbs was less effective, yielding only 35% of the product. Coprecipitation of the starting material **1** was often observed; in this cases, separation of the two products could be performed under the microscope rather easily, crystals of **1** being light orange and those of **2** deep red. Anal. Calcd for C$_6$H$_{18}$Cl$_3$O$_3$RhS$_3$ (M_r = 443.64): C, 16.24; H, 4.08; Cl, 23.97; S, 21.67. Found: C, 16.1; H, 3.97; Cl, 24.04; S, 21.8. Visible spectra (λ_{max}, nm (ϵ, M^{-1} cm^{-1})): in CHCl$_3$ solution, 405 (256), 510 (sh, br, 40); in H$_2$O solution, 409 (230), 490 (sh, br, 45); in DMSO solution, 400 (sh, 305), 500 (sh, br, 50).

***mer,cis*-RhCl$_3$(DM*S*O)$_2$(Me$_3$Bzm) (3).** A 0.2-g amount of **1** (0.43 mmol) was dissolved in 10 mL of CH$_2$Cl$_2$ and 0.08 g of Me$_3$Bzm (0.5 mmol) added. The orange solution was reacted overnight at room temperature and then evaporated to half-volume without warming. A 1-mL volume of diethyl ether was added and the solution cooled to 4 °C. Light orange crystals formed in 24 h and were filtered off, washed with diethyl ether, and vacuum dried at room temperature. Yield: 60%. Crystals of the disubstituted derivative **4** (see below) and of unreacted starting material could be recovered from the concentrated mother liquor. Anal. Calcd for C$_{14}$H$_{24}$N$_2$Cl$_3$O$_2$RhS$_2$ (M_r = 525.74): C, 31.98; H, 4.60; N, 5.33; Cl, 20.23; S, 12.19. Found: C, 31.72; H, 4.58; N, 5.16; Cl, 20.34; S, 12.10. ^{1}H NMR spectrum in CDCl$_3$: 8.44 (s, 1), 8.31 (s, 1), 7.10 (s, 1), 3.82 (s, 3, N–CH$_3$), 3.63 (s, 6, DM*S*O), 3.53 (s, 6, DM*S*O)), 2.38 (s, 3), 2.35 ppm (s, 3). Selected IR absorption bands (KBr): ν_{S-O} 1128 cm^{-1} (br, vs DM*S*O)); ν_{Rh-S} 435 cm^{-1} (m); ν_{Rh-Cl} 346 cm^{-1} (s). Visible spectra (λ_{max}, nm (ϵ, M^{-1} cm^{-1})): in CHCl$_3$ solution, 433.6 (262).

***mer,cis*-RhCl$_3$(Me$_3$Bzm)$_2$(DM*S*O) (4).** A 0.23-g amount of **1** (0.5 mmol) was dissolved in 15 mL of CHCl$_3$ and 0.18 g of Me$_3$Bzm (1.1 mmol) added. The orange solution was reacted overnight at room temperature and then evaporated to approx 5 mL without warming. A small amount of diethyl ether was added and the solution cooled to 4 °C. Orange-yellow crystals of the product formed within 24 h and were then filtered off, washed with diethyl ether, and vacuum dried at room temperature. Yield: 75%. Anal. Calcd for C$_{22}$H$_{30}$N$_4$Cl$_3$ORhS (M_r = 607.83): C, 43.47; H, 4.97; N, 9.21; S, 5.27. Found: C, 43.54; H, 5.06; N, 9.20; S, 5.22. ^{1}H NMR spectrum in CDCl$_3$: 8.47 (s, 1), 8.36 (s, 1), 7.42 (s, 1), 7.06 (s, 1), 7.05 (s, 1), 6.89 (s, 1), 3.81 (s, 3, N–CH$_3$), 3.77 (s, 3, N–CH$_3$), 3.72 (s, 6, DM*S*O), 2.27 (s, 3), 2.26 (s, 3), 2.06 (s, 3), 1.96 ppm (s, 3). Selected IR absorption bands (KBr): ν_{S-O} 1125 cm^{-1} (vs, DM*S*O); ν_{Rh-S} 433 cm^{-1} (m); ν_{Rh-Cl} 341 cm^{-1} (s). Visible spectra (λ_{max}, nm (ϵ, M^{-1} cm^{-1})): in CHCl$_3$ solution, 415 (167).

Table I. Crystallographic Data for *mer,trans*-RhCl$_3$(DM*S*O)$_2$(DMS*O*) (**2**)

formula	C$_6$H$_{18}$Cl$_3$O$_3$RhS$_3$
M_r	443.66
crys system	monoclinic
space group	$P2_1/c$
a (Å)	10.123(6)
b (Å)	13.557(2)
c (Å)	11.109(5)
β (deg)	94.49(2)
V (Å^3)	1520(1)
Z	4
D_{calc} (Mg/m^3)	1.94
diffractometer	Enraf-Nonius CAD4
λ (Å)	0.710 69 (graphite-monochromated Mo Kα)
temp (K)	294 ± 1
μ (cm^{-1})	20.26
cryst size (mm)	0.4 × 0.4 × 0.5
F(000)	888
scan type	$\omega/2\theta$
ω scan rate (deg/min)	1–7
θ range (deg)	2.0–30.0
scan angle[a]	1.1 + 0.35 tan θ
aperture width	1 + tan θ
intensity monitors[b]	3
transm factors	0.949–1.000
data collcd	4601
unique data with $I > 3\sigma(I)$	3192
R[c]	0.048
R_w[d]	0.055
w[e]	$1/[\sigma\|F_o\|^2 + (0.02\|F_o\|)^2 + 1]$
GOF[f]	0.760
resids in final map (e·Å^2)	–2.02, +1.48

[a] Extended by 25% on both sides for background measurements. [b] Measured after each 5000 s. [c] $R = \sum\|\|F_o\| - \|F_c\|\|/\sum\|F_o\|$. [d] $R_w = [\sum w(\|F_o\| - \|F_c\|)^2/\sum w\|F_o\|^2]^{1/2}$. [e] Killean, R. C. G.; Lawrence, J. L. *Acta Crystallogr.* **1969**, *B25*, 1750. [f] GOF = $[\sum w(\|F_o\| - \|F_c\|)^2/(m - n)]^{1/2}$; m = no. of observables, n = no. of variables.

***mer,trans*-RhCl$_3$(DM*S*O)(Me$_3$Bzm)(DMS*O*) (5).** A 0.15-g amount of **2** (0.34 mmol) was dissolved in 15 mL of acetone and 0.11 g of Me$_3$Bzm (0.68 mmol) added. The orange-red solution was reacted for 30 min at room temperature, and then it was evaporated to approximately half-volume without warming and stored at 4 °C after addition of 3 mL of diethyl ether. Orange-yellow microcrystals of the product formed within a few hours. They were filtered off, washed with diethyl ether, and vacuum dried at room temperature. Yield: 40%. A mixture of **3** and **4** could be recovered from the concentrated mother liquor. Anal. Calcd for C$_{14}$H$_{24}$N$_2$Cl$_3$O$_2$RhS$_2$ (M_w = 525.74): C, 31.98; H, 4.60; N, 5.33; S, 12.19. Found: C, 31.6; H, 4.49; N, 5.29; S, 12.02. ^{1}H NMR spectrum in CDCl$_3$: 8.49 (s, 1), 8.19 (s, 1), 7.18 (s, 1), 3.90 (s, 3, N–CH$_3$), 3.62 (s, 6, DM*S*O), 2.61 (s, 6, DMS*O*), 2.39 (s, 3), 2.37 ppm (s, 3). Selected IR absorption bands (KBr): ν_{SO} 1136 cm^{-1} (vs, DM*S*O); ν_{SO} 910 cm^{-1} (vs, DMS*O*); ν_{Rh-O} 488 cm^{-1} (m); ν_{Rh-S} 432 cm^{-1} (m); ν_{Rh-Cl} 345 cm^{-1} (s). Visible spectra (λ_{max}, nm (ϵ, M^{-1} cm^{-1})): in CHCl$_3$ solution, 416 (204), 496 (sh, br, 45).

Crystallographic Study. Crystals of **2** grew from the concentrated reaction mixture kept at 4 °C. Lattice parameters were determined by least-squares methods from the setting angles of 25 accurately centered reflections on an Enraf-Nonius Cad-4 diffractometer. A summary of the crystal data and details of the intensity data collection and refinement are given in Table I. Intensities were corrected for the gain (17%) observed in the intensities of the three standard reflections, monitored periodically during data collection. An empirical absorption correction, based on ψ scans of three close-to-axial reflections, was applied. The structure was solved by Patterson and Fourier methods. Hydrogen atoms were included at calculated positions and held fixed during least-squares refinement, with $B = 1.3B_{eq}$ of the bonded carbon atom. Refinement with anisotropic temperature factors for non-hydrogen atoms converged to the conventional agreement indices given in Table I. All computations were performed by MolEN[28] on a Micro-VAX 2000 computer. Neutral atomic scattering

---

(28) *MolEN. An Interactive Intelligent System for Crystal Structure Analysis*; Enraf-Nonius: Delft, The Netherlands, 1990.

Table II. Positional Parameters and *B* Values with Estimated Standard Deviations

	x	*y*	*z*	B_{eq} (Å^2)[a]
Rh	0.7738(1)	0.9947(1)	0.7247(1)	2.85(1)
Cl1	0.7522(2)	1.0857(1)	0.5451(1)	4.05(3)
Cl2	1.0024(1)	0.9904(1)	0.7298(2)	4.06(3)
Cl3	0.7783(2)	0.9035(1)	0.9027(1)	4.20(3)
S1	0.7880(2)	1.1384(1)	0.8360(1)	3.51(3)
S2	0.4975(1)	0.9915(1)	0.8331(1)	3.76(3)
S3	0.7648(2)	0.8512(1)	0.6114(2)	3.69(3)
O1	0.6602(4)	1.1758(3)	0.8698(5)	4.7(1)
O2	0.5691(4)	0.9967(3)	0.7154(3)	3.56(8)
O3	0.7938(6)	0.7584(3)	0.6759(5)	5.7(1)
C11	0.8969(8)	1.1270(6)	0.9661(6)	5.2(2)
C12	0.8696(7)	1.2326(5)	0.7595(7)	5.0(2)
C21	0.3527(8)	1.0590(7)	0.7935(8)	6.6(2)
C22	0.4296(9)	0.8718(6)	0.8319(8)	6.6(2)
C31	0.6089(7)	0.8408(6)	0.5295(7)	5.3(2)
C32	0.8693(7)	0.8597(5)	0.4924(6)	4.7(1)

[a] Anisotropically refined atoms are given in the form of the isotropic equivalent displacement parameter defined as $(4/3)[a^2\beta(1,1) + b^2\beta(2,2) + c^2\beta(3,3) + ab(\cos\gamma)\beta(1,2) + ac(\cos\beta)\beta(1,3) + bc(\cos\alpha)\beta(2,3)]$.

Table III. Selected Bond Distances (Å) and Angles (deg)

Rh–Cl1	2.342(2)	S1–C12	1.774(8)
Rh–Cl2	2.312(1)	S2–O2	1.545(4)
Rh–Cl3	2.329(2)	S2–C21	1.754(8)
Rh–S1	2.306(2)	S2–C22	1.763(9)
Rh–S3	2.315(2)	S3–O3	1.465(5)
Rh–O2	2.067(4)	S3–C31	1.765(7)
S1–O1	1.466(5)	S3–C32	1.761(7)
S1–C11	1.755(7)		
Cl1–Rh–Cl2	93.46(6)	Rh–S1–C11	112.1(3)
Cl1–Rh–Cl3	175.79(6)	Rh–S1–C12	111.3(3)
Cl1–Rh–S1	90.53(5)	O1–S1–C11	109.2(3)
Cl1–Rh–S3	89.00(6)	O1–S1–C12	109.1(3)
Cl1–Rh–O2	85.7(1)	C11–S1–C12	99.9(4)
Cl2–Rh–Cl3	90.74(6)	O2–S2–C21	101.7(3)
Cl2–Rh–S1	89.31(6)	O2–S2–C22	104.1(4)
Cl2–Rh–S3	89.35(6)	C21–S2–C22	99.2(4)
Cl2–Rh–O2	178.4(1)	Rh–S3–O3	117.2(2)
Cl3–Rh–S1	89.84(6)	Rh–S3–C31	110.0(3)
Cl3–Rh–S3	90.72(6)	Rh–S3–C32	110.7(2)
Cl3–Rh–O2	90.1(1)	O3–S3–C31	108.7(4)
S1–Rh–S3	178.55(6)	O3–S3–C32	108.3(3)
S1–Rh–O2	92.1(1)	C31–S3–C32	100.6(3)
S3–Rh–O2	89.3(1)	Rh–O2–S2	119.5(2)
Rh–S1–O1	114.3(2)		

factors and anomalous dispersion terms were taken from ref 29. Atomic parameters are reported in Table II; bond lengths and angles, in Table III.

Results

We found that, upon irradiation with solar light of a $CDCl_3$ solution of **1** (Figure 1), two new singlets in a 2:1 ratio grew in the ^1H NMR spectrum at 3.53 ppm (DM*S*O) and 2.78 ppm (DMS*O*) at the expense of the original signals of **1** (Table IV).[30] The new resonances, which correspond to those of the minor species already evidenced in previous NMR studies of **1**,[8,9] could be unambiguously attributed to the new linkage isomer *mer,trans*-$RhCl_3$(DM*S*O)$_2$(DMS*O*) (**2**) (Figure 1). In fact, two equally intense signals in the S-bonded region would be expected for the less symmetric *fac*-$RhCl_3$(DM*S*O)$_2$(DMS*O*) isomer (**2a**).[8,9] An equilibrium mixture of **1** and **2** (approximately 1:3), was eventually reached after 2 h of exposure of the NMR tube to sunlight. The new linkage isomer could be prepared in good yield by irradiation of concentrated acetone solutions of **1**, either with solar or artificial light. In agreement with the proposed geometry, the IR spectrum of **2** was very similar to that of the corresponding Ru(III) analogue (**2Ru**) already reported by us.[24] The visible spectrum of **2** is characterized by two rather weak absorptions in the visible range than can be assigned to transitions from the $^1A_{1g}$ ground state to $^1T_{1g}$ and $^1T_{2g}$ upper states.[31] The lower energy band seems to be characteristic of trans S-bonded DMSO ligands, since a very similar one is present also in the spectrum of X[*trans*-$RhCl_4$(DM*S*O)$_2$] compounds.

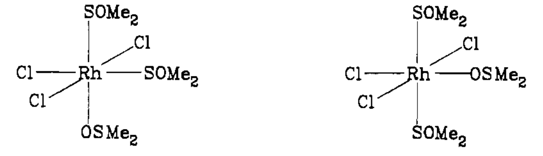
1 2

Figure 1. Schematic structural features of *mer,cis*-$RhCl_3$(DM*S*O)$_2$(DMS*O*) (**1**) and *mer,trans*-$RhCl_3$(DM*S*O)$_2$(DMS*O*) (**2**).

Table IV. Spectroscopic Features of Complexes *mer,cis*-$RhCl_3$(DM*S*O)$_2$(DMS*O*) (**1**), *mer,trans*-$RhCl_3$(DM*S*O)$_2$(DMS*O*) (**2**), and *mer,trans*-$RuCl_3$(DM*S*O)$_2$(DMS*O*) (**2Ru**)

	1		**2**		**2Ru**[a]	
	DM*S*O	DMS*O*	DM*S*O	DMS*O*	DM*S*O	DMS*O*
			^1H NMR (ppm)			
$CDCl_3$	3.63 (6H)[b] 3.44 (6H)[c]	2.87 (6H)	3.54 (12H)	2.78 (6H)	−10 (br)[d]	9 (br)
CD_2Cl_2	3.56 (6H)[b] 3.37 (6H)[c]	2.81 (6H)	3.45 (12H)	2.72 (6H)		
D_2O[e]	3.59 (6H)[b] 3.41 (6H)[c]	2.90 (6H)	3.58 (6H) 2.71 (6H) (free)	2.84 (6H)	−15 (br) 2.71 (free)	9 (br)
			^{13}C NMR[f] (ppm)			
$CDCl_3$	46.2 41.8	38.3	41.5	37.6		
CD_2Cl_2	46.4 42.1	38.6	41.8	37.9		
			IR (KBr, cm^{-1})			
ν_{S-O}	1148 (vs) 1131 (vs)	934 (vs)	1140 (vs) 1120 (vs)	911 (vs)	1127 (vs) 1107 (vs)	912 (vs)
ν_{M-O}		492 (m)		506 (m)		496 (m)
ν_{M-S}	425 (m)		415 (s)		411 (m)	
ν_{M-Cl}	355 (vs) 345 (s) 333 (s)		349 (vs)		342 (vs)	

[a] See also ref 24. [b] Trans to DMSO. [c] Cis to DMS*O*; see also refs 8 and 9. [d] br, broad; m, medium; s, strong; vs, very strong. [e] Soon after dissolution. [f] See also ref 22.

Single-crystal X-ray investigation (Figure 2) confirmed that **2** is isostructural with the ruthenium derivative **2Ru**.[24] Bond lengths and angles involving the DMSO molecules in **2** (Table III) compare rather well with those of **2Ru** and are in the usual ranges for S- and O-bonded DMSO ligands. A significant increase of the Rh–S bond lengths is observed in **2** (average 2.311(6) Å) compared to **1** (average 2.243(16) Å); this trend is paralleled by the decrease of the Rh–S stretching frequencies (Table IV). Unfortunately, the structure determination of **1**[20] is of very low accuracy ($R = 0.125$) so that minor differences in the structural parameters of the two Rh isomers cannot be fully discussed.

The chemical behavior of the new isomer has been investigated both in protic and aprotic solvents. In aqueous solution **2** behaves similarly to **2Ru**[24] and, as indicated by ^1H NMR (Table IV), it readily dissociates one of the two trans S-bonded DMSO

---

(29) *International Tables for X-ray Crystallography*; Kynoch: Birmingham, England, 1974; Vol. IV, Tables 2.2 A and 2.3.1.

(30) Note: Beside the presence of the all S-bonded isomer, the $CDCl_3$ spectrum of **1** can be further complicated by the presence of two peaks of equal intensity at 3.68 and 3.50 ppm, sometimes accompanied by an equally intense peak for free DMSO. These peaks are attributed to the aquo derivative *mer,cis*-$RuCl_3$(DM*S*O)$_2$(H_2O) (**1·H$_2$O**), either derived from partial hydrolysis of the O-bonded DMSO or present as an impurity of **1**. The attribution was confirmed by the $CDCl_3$ spectrum of pure **1·H$_2$O** isolated in the synthesis of **1**. The signals of **1·H$_2$O** shift slightly downfield upon increasing the water content in $CDCl_3$, so that the upfield peak can sometime overlap the minor peak of the all S-bonded isomer.

(31) Cotton, F. A.; Wilkinson, G. *Advanced Inorganic Chemistry*, 5th ed.; John Wiley & Sons: Toronto, Canada, 1988; p 909.

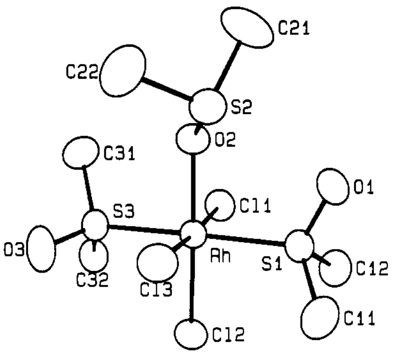

Figure 2. ORTEP drawing of *mer,trans*-$RhCl_3$(DM*S*O)$_2$(DMS*O*) (**2**) with the atom-labeling scheme.

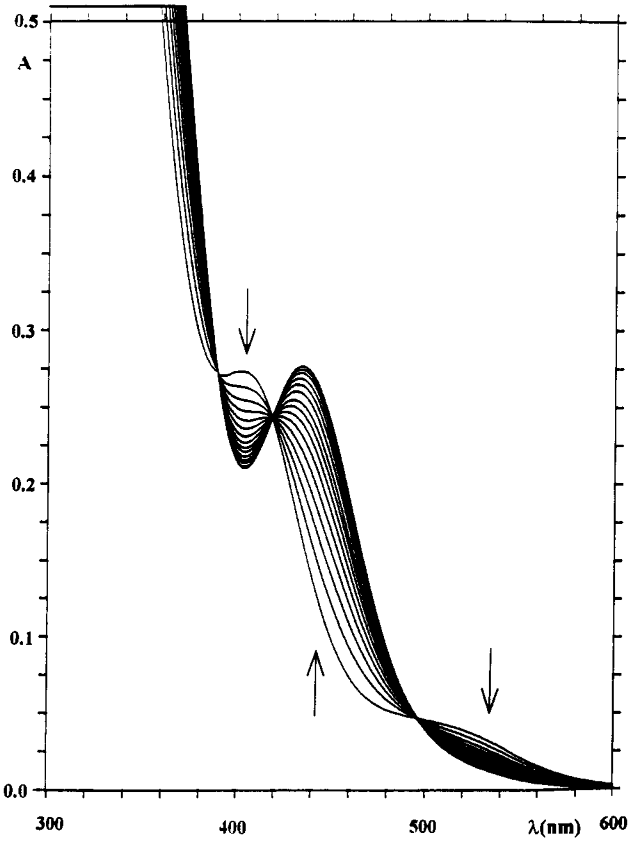

Figure 3. Spectral changes observed in DMSO solution during the thermal isomerization of **2** to **1**. [**2**] = 1×10^{-3} M, $T = 50$ °C, and scan-time interval = 90 min.

molecules, producing the corresponding aquo derivatives. No signals of the parent compound could be found. On the contrary, upon dissolution of **1** in water, dissociation of the O-bonded DMSO occurs. The process is however slow enough to allow determination of the chemical shifts of **1**.

In aprotic solvents **2** is thermodynamically unstable with respect to **1** and it slowly isomerizes with first-order kinetics. This isomerization has been followed spectrophotometrically in dimethyl sulfoxide solution (Figure 3), where, according to the final spectral pattern, it is complete. The three neat isosbestic points suggest that during the process only the two species **1** and **2** are present in solution. The rate constants have been determined at five temperatures in the range 40–65 °C (supplementary material), and the activation parameters were calculated: $\Delta H^{*} = 86 \pm 3$ kJ/mol; $\Delta S^{*} = -61 \pm 8$ J/(mol·K); $k_{25\,°C} = 2.56 \times 10^{-6}$ s^{-1}. On the other hand, according to ^{1}H NMR the thermal isomerization of **2** in chloroform slowly leads (approximately 3 days at 25 °C) to an equilibrium mixture of the two isomers (90% of **1**). A small amount of free DMSO could be also detected at equilibrium, together with the signals of the all S-bonded isomer.[8,9] The same equilibrium ratio could be eventually reached in longer times from a solution of **1** kept in the dark.[8,9]

Scheme I. Reactivity of **1** and **2** with Nitrogen Donor Ligands (N)

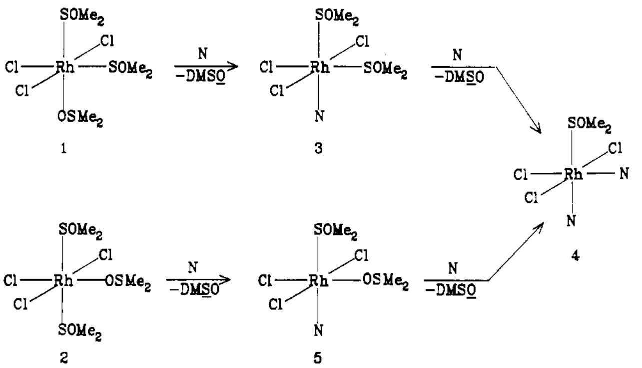

Table V. Spectroscopic Features of *mer,cis*-$RhCl_3$(DM*S*O)$_2$(Me_3Bzm) (**3**), *mer,trans*-$RhCl_3$(DM*S*O)(Me_3Bzm)(DMS*O*) (**5**), and *mer,trans*-$RuCl_3$(DM*S*O)(Me_3Bzm)(DMS*O*) (**5Ru**)

	3		**5**		**5Ru**	
	DM*S*O	DMS*O*	DM*S*O	DMS*O*	DM*S*O	DMS*O*
			^{1}H NMR (ppm)			
$CDCl_3$	3.63 (6H) 3.53 (6H)		3.62 (6H)	2.61 (6H)		
			IR (KBr, cm^{-1})			
ν_{S-O}	1128 (br, vs)[a]		1136 (vs)	910 (vs)	1094 (vs)	926 (vs)
ν_{M-O}				488 (m)		495 (m)
ν_{M-S}	435 (m)		432 (m)		425 (m)	
ν_{M-Cl}	346 (s)		345 (s)		331 (s)	

[a] br, broad; m, medium; s, strong; vs, very strong.

The thermal isomerization of **2** in aprotic solvents is slow enough at room temperature to allow reaction of the complex with uncharged ligands. In particular, we compared the reactivity of **1** and **2** with the nitrogen donor ligand 1,5,6-trimethylbenzimidazole (Me_3Bzm) (Scheme I). Reactions were followed by ^{1}H NMR spectroscopy, and the products were isolated and characterized. As expected,[9] when treated with a slight excess of Me_3Bzm at room temperature, **1** readily replaces the O-bonded DMSO to give *mer,cis*-$RhCl_3$(DM*S*O)$_2$(Me_3Bzm) (**3**). Beside the signals of the coordinated nitrogen ligand, the $CDCl_3$ ^{1}H NMR spectrum of **3** has two singlets in the S-bonded region, accounting for 6 protons each (Table V), that were attributed to the equivalent methyl groups of the two inequivalent DM*S*O ligands. The only other isomer that would give a similar NMR pattern is *fac*-$RhCl_3$(DM*S*O)$_2$(Me_3Bzm) (**3a**), where the two equivalent DM*S*O ligands have inequivalent methyl groups. Formation of **3a** would however require the mer to fac isomerization of the three chlorides, in disagreement with the known structures of other monosubstituted derivatives of **1** that are all of the type *mer,cis*-$RuCl_3$(DM*S*O)$_2$(L).[10–12] The last possible isomer, *mer,trans*-$RhCl_3$(DM*S*O)$_2$(Me_3Bzm) (**3b**), would instead give only one resonance for the equivalent DMSO ligands. The geometry of **3** was further supported by NOE experiments. In fact, NOE enhancement was observed only between the DM*S*O resonance at 3.53 ppm and the two aromatic signals of Me_3Bzm at 8.44 and 8.31 ppm, presumably H2 and H7. This result suggests that only the DMSO that resonates at 3.53 ppm is cis to Me_3Bzm, while the other one is trans to it. In the case of isomer **3a**, both DMSO ligands would be cis to Me_3Bzm and might be expected to give NOE enhancement with some of its signals.

When either **3** was reacted with Me_3Bzm or the reaction of **1** was carried out with excess of Me_3Bzm, formation of *mer,cis*-$RhCl_3$(Me_3Bzm)$_2$(DM*S*O) (**4**) upon replacement of a further DM*S*O was observed. The geometry of **4** could be unambiguously established from the ^{1}H NMR spectrum that showed two sets of

Scheme II. Proposed Mechanism for the Thermal Reversible Isomerization of **2** and **1** and for Their Stereospecific Reactivity with Neutral Ligands (L)

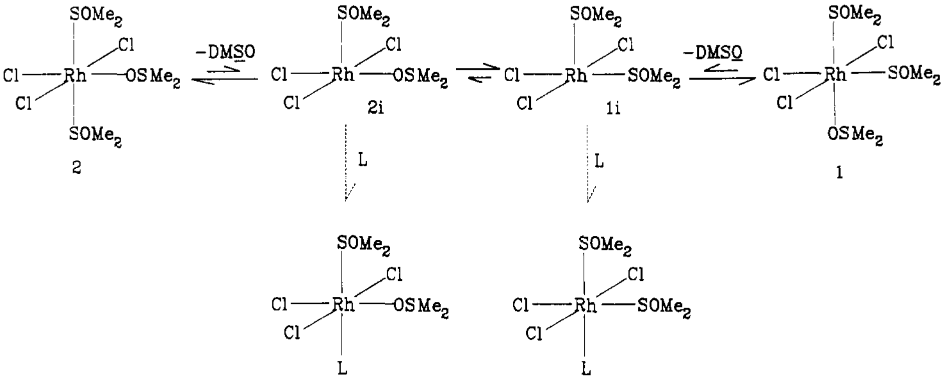

signals for the two Me_3Bzm ligands and one singlet at 3.72 ppm for the remaining DMS*O*. Only one set of signals for the two nitrogen ligands would be expected for the other two possible isomers, that is *mer,trans*-$RhCl_3(Me_3Bzm)_2$(DMS*O*) (**4a**) and *fac*-$RhCl_3(Me_3Bzm)_2$(DMS*O*) (**4b**). A derivative similar to **4**, *mer,cis*-$RhCl_3(py)_2$(DMS*O*), has also been reported and structurally characterized.[13]

Reaction of **2** with Me_3Bzm (Scheme I) involves, as a first step, the substitution of one of the two trans S-bonded DMSO ligands with formation of *mer,trans*-$RhCl_3$(DMSO)(Me_3Bzm)(DMS*O*) (**5**), which is a linkage isomer of **3**. The presence of both S-bonded and O-bonded DMSO in **5** was indicated by IR and ^{1}H NMR spectroscopy (Table V). Each of the three different geometries with a *mer* arrangement of the three chlorides, that is also *mer,trans*-$RhCl_3$(DMS*O*)(Me_3Bzm)(DMSO) (**5a**) and *mer,trans*-$RhCl_3$(DMSO)(DMS*O*)(Me_3Bzm) (**5b**), might be in agreement with the observed NMR spectrum; a fac derivative can be excluded, since four signals for the inequivalent methyl groups would be expected. However, NOE enhancement was observed only between the O-bonded DMSO resonance at 2.61 ppm and the aromatic signal of Me_3Bzm at 8.18 ppm (presumably either H2 or H7), thus ruling out isomer **5a**. Formation of **5b** is unlikely since, as in the case of **3**, an NOE enhancement would be expected also between the nitrogen ligand and the cis S-bonded DMSO. On the contrary, formation of **5** does not involve any isomerization in **2** and is in agreement with the reactivity of the analogous Ru(III) derivative.[25] In fact, a *mer,trans*-$RuCl_3$(DMSO)(Me_3Bzm)(DMS*O*) complex (**5Ru**) (Table V) could be easily synthesized upon reaction of **2Ru** with Me_3Bzm according to the procedure reported for other nitrogen ligands.[25]

Isomers **1** and **2** reacted in a similar fashion with gaseous ammonia to give *mer,cis*-$RhCl_3(DMSO)_2(NH_3)$ (**6**) and *mer,trans*-$RhCl_3$(DMSO)(NH_3)(DMS*O*) (**7**), respectively (supplementary material). In this case, precipitation of the monosubstituted derivatives from the reaction medium prevented formation of the disubstituted product.

Discussion

Compounds **1** and **2** can be also regarded, in a more general sense, as geometric isomers. However, since in the isomerization process the overall geometry of the alike ligands remains unchanged (i.e. mer), we prefer to adopt their original definition of linkage isomers.[8] To the best of our knowledge, this is the first example where the structures of two isomers differing only in the binding mode of the DMSO ligands are known. In the previous reports, the S/O isomerization was either accompanied by a rearrangement in the geometry of the complex (e.g. *cis*-$RuCl_2(DMSO)_3$(DMS*O*) and *trans*-$RuCl_2$(DMS*O*)$_4$)[23] or was induced by a change in the nature of the sulfoxide (e.g. *cis*-$RuCl_2(DMSO)_3$(DMS*O*) and *cis*-$RuCl_2(TMSO)_4$) (TMSO = tetramethylene sulfoxide))[32] or in the nature of other ligands (e.g. $Rh_2(O_2CCH_3)_4(DMSO)_2$ and $Rh_2(O_2CCF_3)_4$(DMS*O*)$_2$).[33]

The definition of linkage isomers for **1** and **2** is also in agreement with the following proposed isomerization mechanism. According to NMR data, in aprotic solvents such as chloroform the thermal isomerization of **2** to **1** is reversible. A proposed mechanism must therefore account for common intermediate species. In agreement with the observation that the chemical behavior of **1** and **2** in solution is dominated by the rather strong trans-effect of S-bonded DMSO,[34] a mechanism involving as a first step the dissociation of one of the two trans DMSO ligands can be reasonably proposed (Scheme II). Dissociation of a DMSO from **2** and of a DMS*O* from **1** will produce the two isomeric square pyramidal intermediates **2i** and **1i**, respectively. Even though there is no spectroscopic evidence for **2i** and **1i**, their formation is supported by the reactivity of **1** and **2** with uncharged ligands, which can be explained as a trapping of the intermediates (Scheme II). Due to the stereoselectivity observed in those reactions, a major geometric rearrangement of the intermediates is rather unlikely. The S/O linkage isomerization step, required by the principle of microscopic reversibility, might occur between **1i** and **2i**. This step is very likely rate determining, in agreement also with the negative entropy of activation measured in DMSO. A positive ΔS^* would be expected for a rate-determining dissociation step.[23] The effect of light might be that of promoting the S to O linkage isomerization step.

The lower thermodynamic stability of **2** compared to **1** is in agreement with what was observed with platinum group metals, where, due to the trans-influencing effect of DMSO,[34] a cis arrangement of two S-bonded DMSO ligands is generally preferred over a trans geometry, even though this latter is sterically less demanding.[8,34,35] From our results it appears that, while the neutral Rh(III) isomers **1** and **2** follow the expected trend, this is not the case for Ru(III), where only the trans DMSO complex **2Ru** has been observed to date. Since difference in ionic size between Rh(III) and Ru(III) is rather negligible (0.015 Å),[36] the reason for this preference of Ru(III) must be electronic rather than steric and lay in the nature of the metal–DMSO bond. S-bonded DMSO is usually considered as a weak π-acceptor.[34] The data reported in our previous papers[23-25] supported a model for the binding of DMSO to ruthenium that involved a π-back-bonding contribution, not only from Ru(II) but also from Ru(III) centers. Ru(III), having a partially filled t_{2g} orbital, might be expected to behave rather like a π-acceptor. Indeed, even though pentaammineruthenium(III) has been reported to be a

---

(32) Alessio, E.; Milani, B.; Mestroni, G.; Calligaris, M.; Faleschini, P.; Attia, W. M. *Inorg. Chim. Acta* **1990**, *177*, 255.
(33) Cotton, F. A.; Felthouse, T. R. *Inorg. Chem.* **1980**, *19*, 2347.
(34) Davies, J. A. *Adv. Inorg. Chem. Radiochem.* **1981**, *24*, 115.
(35) Price, J. H.; Williamson, A. N.; Schramm, R. F.; Wayland, B. B. *Inorg. Chem.* **1972**, *11*, 1280.
(36) Shannon, R. D. *Acta Crystallogr.* **1976**, *A32*, 751.

π-acceptor toward nitriles,[31] detailed structural, spectroscopic, and computational investigations have shown that it is instead a very poor π-acceptor toward ligands such as imidazole and thioethers.[37,38] On the other hand, the electronegative oxygen atom on sulfur is expected to enhance the π-back-bonding ability of DMSO compared to thioethers,[33] and therefore a π-back-bonding contribution in the Ru(III)–DM*S*O bond should not be unexpected. Any increase of this contribution, while reinforcing the Ru–S bond, induces a weakening of the S–O bond.[34] On the other hand, in a pure σ model, a strengthening of the M–S bond would involve a contemporary reinforcement of the S–O bond. The following structural and spectroscopic data, even though they may not be regarded as conclusive, suggest that the Rh(III)–DM*S*O bond is essentially σ in character and exclude significant π-back-bonding contributions: (i) The shortening of the M–S bond length observed on going from **2Ru** to **2** (average 0.030(8) Å) is accompanied by a slight contraction of the S–O bond distance (average 0.014(6) Å). Consistent variations in the M–S and S–O stretching frequencies in **2** and **2Ru** are observed (Table IV). (ii) Replacement of a DM*S*O with a pure σ donor ligand such as Me$_3$Bzm induces different changes in the S–O and M–S stretching frequencies of the remaining DM*S*O in **2** and **2Ru** (cf. Tables IV and V). In fact, while in **2** such replacement involves a contemporary strengthening of the Rh–S bond (ν_{Rh-S} 432 cm^{-1} in **5** vs 415 cm^{-1} in **2**) and of the S–O bond (ν_{S-O} 1136 cm^{-1} in **5** vs 1140 vs 1120 cm^{-1} in **2**), in **2Ru** the strengthening of the Ru–S bond (ν_{Ru-S} 425 cm^{-1} in **5Ru** vs 411 cm^{-1} in **2Ru**) is accompanied by a weakening of the S–O bond (ν_{S-O} 1094 cm^{-1} in **5Ru** vs 1127 and 1107 cm^{-1} in **2Ru**).

Further support to the above hypothesis comes from the comparison of the C–O stretching frequencies in [M(CO)X$_5$]$^{2-}$ complexes.[39] For X = Cl, ν_{CO} = 2117 cm^{-1} for Rh vs 2030 cm^{-1} for Ru, and similarly, for X = Br, ν_{CO} = 2067 cm^{-1} for Rh vs 1996 cm^{-1} for Ru. The higher values in the Rh derivatives imply less π-back-donation from metal orbitals to antibonding C–O MO's. The experimental observation that Rh(III) has a lower π-back-bonding ability than Ru(III) is in agreement with the expected trend in the energy of the metal orbitals due to the increase of the effective nuclear charge going from Ru(III) to Rh(III).

Conclusions

The synthesis and characterization of the new linkage isomer of RhCl$_3$(DMSO)$_3$ described in this paper is a contribution toward the elucidation of the chemistry of rhodium–dimethyl sulfoxide–halide complexes, which is complicated by the possibility for every complex to give geometric and linkage isomers. The rather unique availability of the structural and spectroscopic features of the two Rh linkage isomers **1** and **2**, as well as of **2Ru** and of their substituted derivatives, allowed us to draw some considerations about the Rh–DMSO bonding mode. The photochemical procedure adopted for the synthesis of **2**, together with the previously described photochemical synthesis of *trans*-RuCl$_2$(DM*S*O)$_4$,[23] suggests that the effect of light on rhodium– and ruthenium–DMSO complexes is a topic still largely unexplored that deserves further careful investigation.

2 reacts stereospecifically with neutral ligands to give unprecedented monosubstituted derivatives that are linkage isomers of those obtained from **1**.

The lower thermodynamic stability of **2** compared to **1**, attributed to the unfavorable geometry of the two trans-influencing DM*S*O ligands, suggests that also in the case of the anionic derivative *trans*-[RhCl$_4$(DM*S*O)$_2$]$^-$ a cis isomer of comparable, or even greater, stability might be expected. To date, the existence of *cis*-[RhCl$_4$(DM*S*O)$_2$]$^-$ has been reported only in solution, while a species of this geometry was described in the case of Ir(III).[40,41]

Acknowledgment. This work was supported by the Italian Ministry for University and Scientific and Technological Research (40% grant). Technical support by Mr. P. de Baseggio (Department of Chemical Sciences, University of Trieste) is thankfully acknowledged.

Supplementary Material Available: Tables of anisotropic temperature factors for non-hydrogen atoms, positional and thermal parameters for hydrogen atoms, and kinetic constants and text describing synthetic procedures and spectroscopic data for *mer,cis*-RhCl$_3$(DM*S*O)$_2$(NH$_3$) (**6**) and *mer,trans*-RhCl$_3$(DM*S*O)(NH$_3$)(DMS*O*) (**7**) (5 pages). Ordering information is given on any current masthead page.

---

(37) Krogh-Jespersen, K.; Westbrook, J. D.; Potenza, J. A.; Schugar, H. J. *J. Am. Chem. Soc.* **1987**, *109*, 7025.

(38) Krogh-Jespersen, K.; Zhang, X.; Westbrook, J. D.; Fikar, R.; Nayak, K.; Kwik, W. L.; Potenza, J. A.; Schugar, H. J. *J. Am. Chem. Soc.* **1989**, *111*, 4082.

(39) Cleare, M. J.; Fritz, H. P.; Griffith, W. P. *Spectrochim. Acta* **1972**, *28A*, 2019.

(40) Haddad, Y. M. Y.; Henbest, H. B.; Trocha-Grimshaw, J. *J. Chem. Soc., Perkin Trans. 1* **1973**, 592.

(41) James, B. R.; Morris, R. H.; Kvintovics, P. *Can. J. Chem.* **1986**, *64*, 897.